Transport and ac susceptibility measurements on silver wrapped pellets of $Bi_{1.7}Pb_{0.35}Sr_{1.9}Ca_{2.1}Cu_3O_y$ superconductors

To cite this article: C Terzioglu *et al* 2009 *J. Phys.: Conf. Ser.* **153** 012029

Journal of Physics: Conference Series **153** (2009) 012029 doi:10.1088/1742-6596/153/1/012029

Transport and ac susceptibility measurements on silver wrapped pellets of $Bi_{1.7}Pb_{0.35}Sr_{1.9}Ca_{2.1}Cu_3O_y$ superconductors

C Terzioglu[1], **D Yegen**[2], **A Varilci**[1], **I Belenli**[1]
[1] Department of Physics, Faculty of Arts and Sciences, Abant Izzet Baysal University, 14280 Bolu-Turkey,
[2] Department of Medical Physics, Dr.A.Y. Ankara Oncology Education & Research Hospital, Ministry of Healthy of Turkey, 06460 Ankara, Turkey.

E-mail: terzioglu_c@ibu.edu.tr

Abstract. The effect of the cooling rates on oxygen content of silver sheathed Bi-2223 bulk superconducting samples was investigated performing dc electrical resistivity, transport critical current density, ac susceptibility and x-ray diffraction (XRD) measurements. The bulk samples with Ag sheathing were annealed under identical conditions and cooled with rates of $25^\circ C/h$, $50^\circ C/h$, $75^\circ C/h$, and $100^\circ C/h$. We estimated the transition temperatures from both dc resistivity and ac susceptibility as a function of temperature measurements. It is observed that T_c and J_c depend on cooling rates of the samples. T_c and J_c decrease with increasing cooling rates. The imaginary part of ac susceptibility measurements is used to calculate inter-granular critical current density using the Bean Model. $J_c(T_p)$ is also seen to decreases with increasing cooling rates. The peak temperature, T_p, in the imaginary part of the ac susceptibility is shifted to a lower temperature with increasing cooling rates as well as increasing ac magnetic fields. The force pinning density decreased with increasing the cooling rates. XRD patterns are given to determine lattice parameter c and obtain information about Bi-2223 and Bi-2212 phases.

1. Introduction

Since the discovery of high-T_c superconductors a large amount of work has been done on Bi(Pb)-Sr-Ca-Cu-O system. It is known that chemical doping and preparation condition play very important roles in high-T_c superconductors. Cooling rates are also important for superconducting properties. This importance is partly due to changing oxygen content during the cooling stage. Thus, it is useful to observe the variation of both the superconducting properties as well as the normal state properties of materials with changing cooling rates in order to understand superconductivity better.

The measurements of ac susceptibility are commonly used to determine magnetic and superconducting properties of materials. In particular, the ac susceptibility measurement is useful in determining the specimen and for distinguishing between inter- and intra-grain properties. At high ac fields, two loss peaks can usually be seen in the imaginary part of susceptibility data; a broad peak at low temperature (coupling losses) due to the motion of inter-granular (Josephson) vortices [1] and a narrower peak

[1] Cabir Terzioglu, Department of Physics, Faculty of Arts and Sciences, Abant Izzet Baysal University, 14280 Bolu-Turkey.

(intrinsic losses) due to the motion of intra-granular Abrikosov vortices near T_c^{onset} [1,2]. These two peaks depend on the sample processing variables as well as the samples composition for the Bi-2223 system [3,4].

The cooling rates reported in the literature range from quenching in liquid nitrogen to controlled cooling as slowly as 1 ^oC/h. Mainly the rates can be classified as quenching to liquid nitrogen temperature, quenching in icy water, quenching in air, fast cooling, uncontrolled furnace cooling (~150 ^oC/h) and controlled cooling (1-100 ^oC/h). Cooling rates following the annealing may have a number of effects on samples. The first effect to be mentioned comes from thermal contraction of the sample and bulk samples, films on substrates and metal-ceramic composites will be differently affected. A second effect is on the oxidization sate of the sample. Another effect worth mentioning is the formation of other phases during cooling stage [5]. Slow cooling rates appear to improve the superconducting properties although they do not affect the phase formation of the Bi-2223 phase provided that the annealing duration is sufficiently long. Fast cooling rates may particularly be more harmful for the composite superconductors where there is an interface between two materials with different thermal expansion coefficients.

In recent years, the cooling rate was found to be an important parameter for optimizing performance of Ag-sheathed Bi-based superconductors [6-8]. It was found that the value of J_c decreases with increasing cooling rate. The effect of cooling rate on transport properties of the samples without silver sheathing has recently been investigated [9]. It was obtained that the values of J_c, T_c, lattice parameter c, and hole concentration were increased with increasing cooling rate.

In this work, we report measurements of electrical resistivity and ac susceptibility as a function of temperature and transport and inter-granular critical current density to investigate the effect of the cooling rates on properties of silver wrapped Bi-2223 bulk superconductors annealed at 830 $^\circ C$ for 48 h and cooled with different cooling rates. Also, XRD analysis is used to characterize microstructures of the sample phases.

2. Experimental details

Production of superconducting powders: Bi_2O_3, PbO, $SrCO_3$, $CaCO_3$ and CuO powders were mixed in appropriate ratios to obtain $Bi_{1.7}Pb_{0.35}Sr_{1.9}Ca_{2.1}Cu_3O_y$ and mixed thoroughly in an agate mortar. The mixture was then calcined in a silver crucible at progressively increasing temperatures up to 820 ^oC for 12 hours durations. Pellets with rectangular shape were prepared by pressing from the calcined precursor under 1 GPa uni-axial pressure. The pelletized tablets were heat treated in a silver crucible in the furnace all together. Annealing of the samples was performed in two steps at 830 ^oC for 48 hours durations. The tablets were ground into ceramic powder and re-pelletized before the second annealing. Pellets were completely wrapped in thin silver sheaths and pressed under 1 GPa pressure. These samples were then heat treated at 835 ^oC for 48 hours. The furnace was heated to the annealing temperature with 100 ^oC per hour heating rate and 25 ^oC/h, 50 ^oC/h, 75 ^oC/h, and 100 ^oC/h. cooling rates were applied after the heat treatment. Silver wrapped samples are coded G25 to G100, numbers referring to cooling speeds in units of hour.

XRD data were taken using a Rigaku D/Max-IIIC diffractometer with CuK_α radiation in the range 2Θ = 4°- 60° with a scan speed of 3° /min and a step increment of 0.02° at room temperature. We obtained XRD patterns of the samples after preparation. Silver sheathing was peeled off before XRD examination and patterns were taken from the samples as bulk tablets. Phase purity and the lattice parameters were determined from XRD patterns. The accuracy in determining the lattice parameter c was ±0.001 Å. The relative volume fractions of the Bi-2223 and Bi-2212 phases were determined from the peak intensities of the same particular reflections, using the following expressions [10,11];

$$f_{(2223)} = \frac{\sum I_{H(hkl)}}{\sum I_{H(hkl)} + \sum I_{L(hkl)}} \qquad (1)$$

$$f_{(2212)} = \frac{\sum I_{L(hkl)}}{\sum I_{H(hkl)} + \sum I_{L(hkl)}} \qquad (2)$$

Here $I_{H(hkl)}$ and $I_{L(hkl)}$ are the intensities of the (hkl) diffraction lines for Bi-2223 and Bi-2212 phases, respectively (Fig.1).

The measurements of dc resistivity were performed with the four-probe method on all the samples annealed at 830 $^{\circ}C$ for 48 h with different cooling rates ($25^{\circ}C/h$, $50^{\circ}C/h$, $75^{\circ}C/h$, and $100^{\circ}C/h.$). We measured temperature (80-130 K) dependence of resistivity for the samples using a 10 mA dc current in a cryostat. Both voltage and current contacts were made with silver paint. The transition temperature, T_c, was determined as the temperature of zero resistivity. Room temperature resistivities were calculated from room temperature I-V curves. The critical current density J_c was determined from the current-voltage characteristics of the samples at 77 K. The critical current I_c was determined as the onset of a voltage with a criterion of 1 $\mu V/cm$, and the J_c was obtained from I_c and the cross sectional area of the samples.

Ac susceptibility measurements on the samples were made using a home made ac susceptometer and a Lock-in amplifier (Stanford Research SR850) [12]. The ac susceptibility as a function of temperature (77–120 K) at fixed ac magnetic field amplitude (H_{ac}) in a range from 40 to 600 A/m was performed at a frequency of 1 kHz. The ac magnetic field was applied along the longest dimension of the samples. From the χ' and χ'' vs. T plots, the values of the T_c^{onset} (diamagnetic onset temperature) and T_p (temperature corresponding to χ'' peak) were obtained. We could observe only one peak in each of the χ'' vs. T plots. Bean critical-state model [13] is used for determination of inter-granular critical current densities, $J_c(T_p)$, from ac susceptibility measurements. The values of $J_c(T_p)$ in our samples were calculated using the Bean model from the acquired data.

3. Results and discussion

Oxygen stoichiometry can be studied in more detail by thermogravimetric techniques [14]. We measured the masses of each tablet before and after heat treatments in order to record any mass changes. Weight measurements of the pellets revealed a systematic change in masses of the pellets. The change in masses of silver sheathed Bi-2223 bulk samples decreases from -0.36% to -0.46% with increasing cooling rates but the samples without silver sheathing lost more mass [8]. Silver wrapped bulk samples may have experienced mass loss due to oxygen loss through silver sheathing and sublimation of silver at high temperatures [15]. It can be interpreted that there is no silver sheathing so that out diffusion of oxygen is faster and sublimation of Pb and Bi is also easier. Since the out diffusion of oxygen does not happen during cooling, the difference can be attributed to loss of oxygen during annealing, and sublimation Bi and Pb. It should be considered that sample's geometry (volume to surface ratio) plays an important role in sublimation and oxygen intake. Film samples are most prone to sublimation and ease of oxygen intake in this respect.

The XRD patterns from the surface of the G25 and G100 samples are shown in Fig. 1. Some of the Miller indices are indicated in the figure. There is no significant increase in the intensities of particular peaks between the G25 and G100 samples. The lattice parameters for the samples with different cooling rates were determined by using a linear least squares method and were tabulated in Table 1. It is observed that the lattice parameter c decreases with increasing cooling rates. In contrary to this, the lattice parameter c increased with increasing cooling rates in the samples without silver sheathing [9]. The impurity phase (Ca_2PbO_4) is observed around $2\theta = 18^{\circ}$ in both samples in which the intensity of the G25 is higher than that of G100.

The relative volume fraction of the samples calculated using Eqs. (1) and (2) is listed in Table 1. In contrast to the samples without silver sheathing, with increasing cooling rates, the volume fraction of Bi-2223 phase increased and that of Bi-2212 phase decreased.

Table 1. Critical temperature T_c, transport critical current density J_c, lattice parameter c, volume fraction, room temperature resistivity, hole concentration, p of the samples.

Samples	T_c^{offset} (K)	Lattice Parameter c (Å)	J_c^{trans} (A/cm^2)	Hole Concentration p	Volume Fraction (%) Bi-2223	Bi-2212	ρ (mΩ.cm) at 300 K
G25	98 ± 0.2	37.195	150	0.124	83	17	5.60
G50	91 ± 0.2	37.187	120	0.114	80	20	7.50
G75	88 ± 0.2	37.180	50	0.111	77	23	11.20
G100	86 ± 0.2	37.175	40	0.109	75	25	13.10

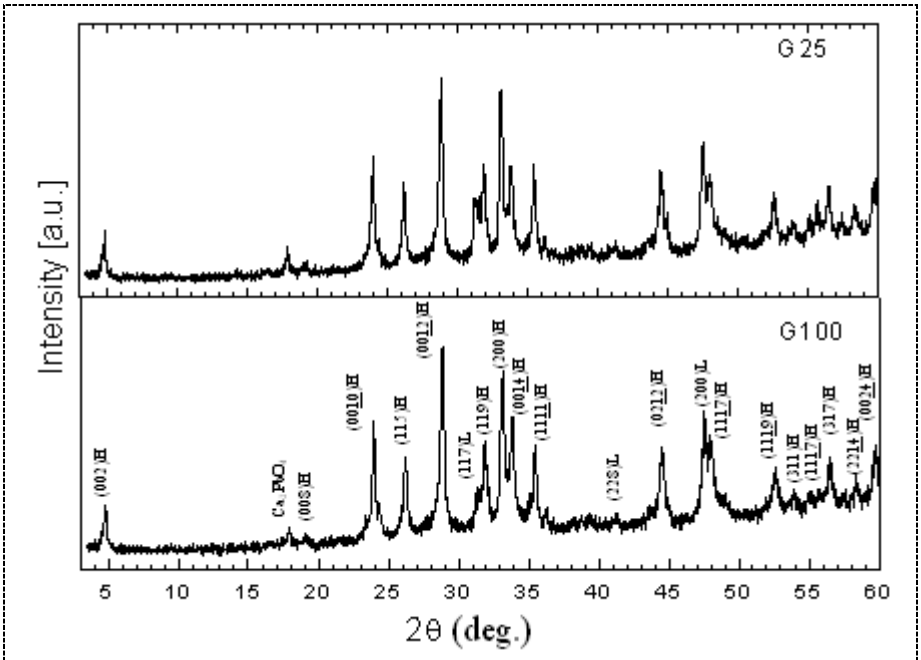

Figure 1. The XRD patterns for the G25 and G100 samples. The peaks indexed (hkl)L and (hkl)H represent the Bi-2212 and Bi-2223 phases respectively.

The electrical resistivity was measured on bar shaped specimens after removal of silver sheathing, using the standard four-probe dc technique, in the temperature range between 80 and 130 K. The temperature dependence of normalized resistivity for all samples annealed at 830 $^{\circ}C$ for 48 h is shown in Fig. 2. Room temperature resistivities were calculated from room temperature I-V curves (Table 1). Every sample shows linear temperature dependence in normal state, characteristic of Cu-oxide-based (high-T_c) superconductors. The resistivity in the normal state increases with increasing cooling rates. The increase of the normal state resistivity is likely to be due to grain boundaries. Zero-resistivity transition temperatures of the G25, G50, G75, and G100 samples are determined to be 98 K, 91 K, 88 K and 86 K, respectively. The transition temperature decreases with increasing cooling rates. It was observed that the slow cooled sample has lower normal state resistivity, higher zero resistivity transition temperature and longer lattice parameter c. It is observed that the resistivity transition width broadens with increasing the cooling rate, from 25 ^{o}C/h to 75 ^{o}C/h. The sample cooled with 100 ^{o}C/h

shows narrower transition but the transition starts at a much lower temperature. As can be seen from the figure, the transition curves from normal to superconducting state indicate double step transition in G50 and G75 samples.

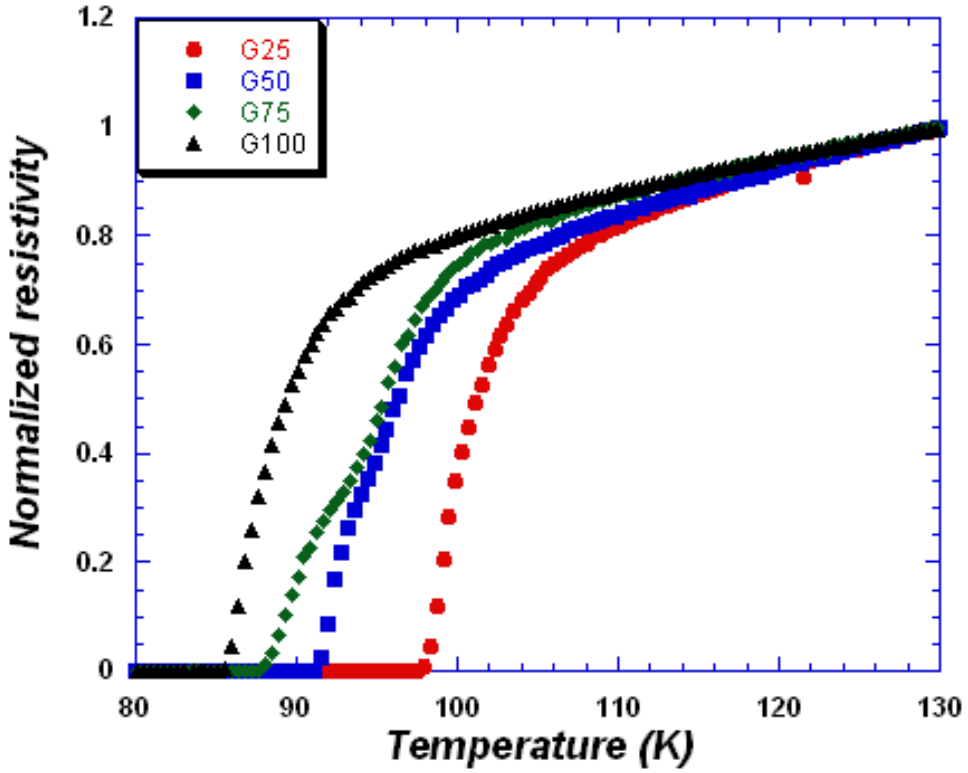

Figure 2. Temperature dependence of normalized resistivity for silver wrapped $Bi_{1.7}Pb_{0.35}Sr_{1.9}Ca_{2.1}Cu_3O_y$ samples annealed at 830 $^\circ C$ for 48 h with cooling rate of 25 $^\circ C$ /h, 50 $^\circ C$ /h, 75 $^\circ C$ /h and 100 $^\circ C$ /h samples.

The transport critical current densities as a function of cooling rates were measured in liquid nitrogen at self magnetic fields. It was observed that the J_c of the samples decreases from 150 A/cm^2 to 40 A/cm^2 with increasing the cooling rates (Table 1). Low values of critical current density are due to bulk nature of our silver sheathed samples rather than silver sheathed tapes. It was concluded that the enhancement of Jc with decreasing cooling rate is due to increase in the flux pinning strength. Tetenbaum and Maroni reported [16] that slow cooling increases the oxygen content of Bi-2223 phase. It was interpreted that this increase in oxygen content may contribute to the enhanced critical current density observed during the slow cooling for the samples with silver sheathing. In contrast to this, the value of Jc of the samples without silver sheathing increases with increasing cooling rate [9].
The carrier (number of holes) concentration, p, is calculated by using the relation [17]

$$T_c/T_c^{max} = 1 - 82.6\,(p - 0.16)^2 \qquad (3)$$

where T_c^{max} is taken as 110 K for Bi-2223 system. This formula is found to be applicable to several cuprate systems [18,19]. The calculated carrier concentration is listed in Table 1. It is observed that hole carrier concentration decreases from 0.124 to 0.109 with decreasing transition temperature (with increasing cooling rates). It is well known that a parabolic relationship holds between the

superconducting transition temperature and hole concentration, being consistent with the present data. The slight increase in T_c with decreasing cooling rate may also be related to the optimization of the hole density. Thus, the cooling rate affects the hole concentration and reduces the carrier density with increasing cooling rates.

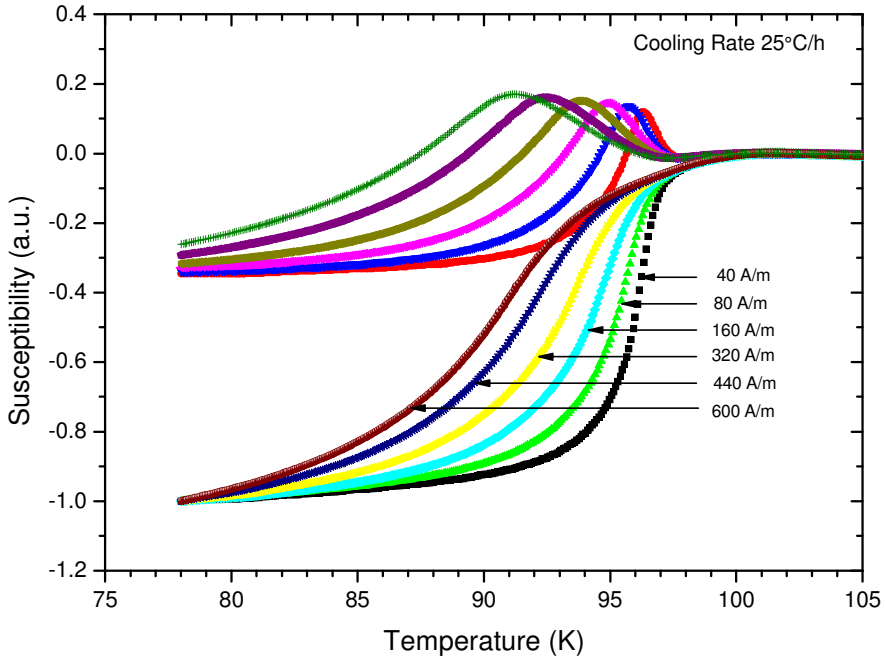

Figure 3. Temperature dependence of the real part and imaginary part of ac susceptibility for silver wrapped $Bi_{1.7}Pb_{0.35}Sr_{1.9}Ca_{2.1}Cu_3O_y$ annealed at 830 $^\circ C$ for 48 h with cooling rate of 25 $^\circ C$ /h sample at different ac field amplitudes.

We have investigated ac susceptibility as a function of temperature under different ac field amplitudes for the samples. χ' measures the amount of shielding and χ'' the amount of energy loss due to the induced current. Fig. 3 represents some characteristic results of ac susceptibility (χ' and χ'') as a function of temperature under different ac fields for 1 kHz for G25 sample. The maximum of χ'' appears at a temperature T_p where the inter-granular field just penetrates the centre of sample [20]. The intensity of the imaginary parts increases with increasing ac field amplitude. At T_p in the imaginary part, ac field amplitude equals to full flux penetration field, H_p. For sintered high-T_c superconductors temperature dependence of the imaginary part of complex ac susceptibility shows two peaks, T_p and T_g, at high ac fields [21]. The first peak (at high field) appears at a temperature T_g slightly bellow T_c^{onset} due to intra-granular supercurrents, and a second loss peak (at low-field) appears at a temperature T_p lower than T_g due to sample-circulating inter-granular supercurrents. We did not see any intrinsic losses peaks in our samples. The absence of intra-grain peak, T_g, is due to the presence of smaller decoupled grain in the samples [22]. The overall susceptibility curves of the samples are shifted to lower temperature by increasing the ac field amplitude. These results suggest that peak temperatures, T_p, shift to lower temperature with increasing ac field amplitudes (Fig. 3). The shift of T_p with field can be explained in terms of the strength of the pinning force. The effective

pinning force density decreases with increasing ac magnetic field causing T_p to shift to lower temperature.

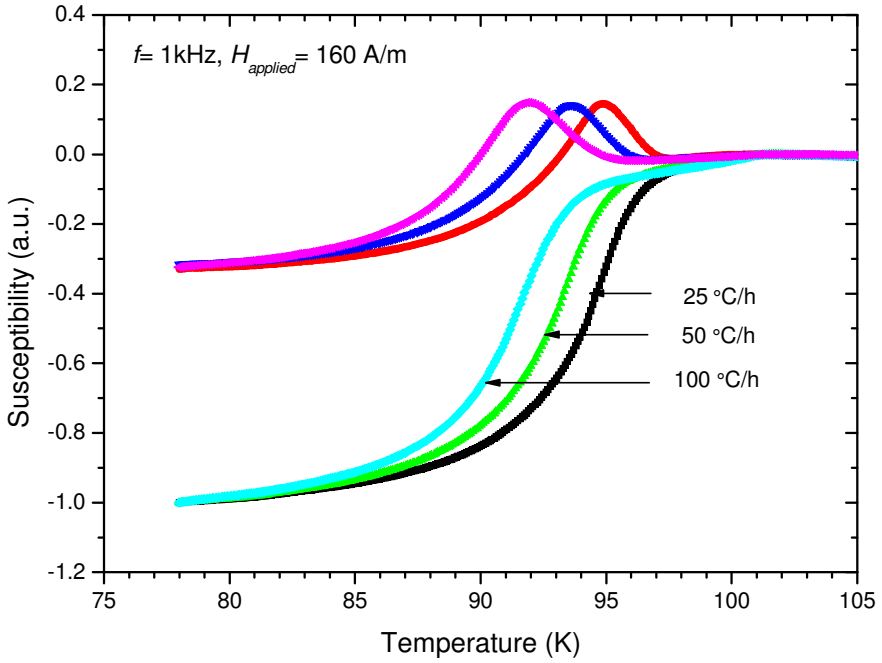

Figure 4. Ac susceptibility ($\chi = \chi' + i\chi''$) versus temperature plots for silver wrapped $Bi_{1.7}Pb_{0.35}Sr_{1.9}Ca_{2.1}Cu_3O_y$ annealed at 830 $^\circ C$ for 48 h with cooling rate of (a) 25 $^\circ C$ /h , (b) 50 $^\circ C$ /h and (c) 100 $^\circ C$ /h samples for H_{ac} = 160 A/m. annealed at 830 $^\circ C$ for 48 h with cooling rate of 25 $^\circ C$ /h sample at different ac field amplitudes.

As can be seen in Fig. 4, the susceptibility-temperature curves shifted to lower temperatures and considerably increased the transition width in χ'' -T curves, and also decreased the shielding fraction of the superconducting phase in the samples with increasing the cooling rates. In another word, the susceptibility curves become sharper with decreasing cooling rate, being in agreement with the literature [6]. The sample cooled slowly with 25°C/h (G25) appears to have the strongest connectivity between grains. The fast cooled one (G100) has the weakest links. If we compare these results with resistivity measurements of Fig. 2, sample G25 has better connectivity between grains and sample G100 has the weakest coupling between grains. The data suggest that the faster cooling rates improve the inter-grain connectivity. The ac susceptibility and dc electrical resistivity measurements show the same behaviour such as the transition width increases with increasing the cooling rates. The real and imaginary parts are zero when the sample is in the normal state. χ'' turns positive due to the extent of increasing flux penetration with decreasing temperature below T_c^{onset}. At T_p, full penetration and maximum peak are observed. Below T_p, the intensity of χ'' falls due to decreasing amount of flux penetration. When the temperature reaches to lowest value the whole body starts to shield.

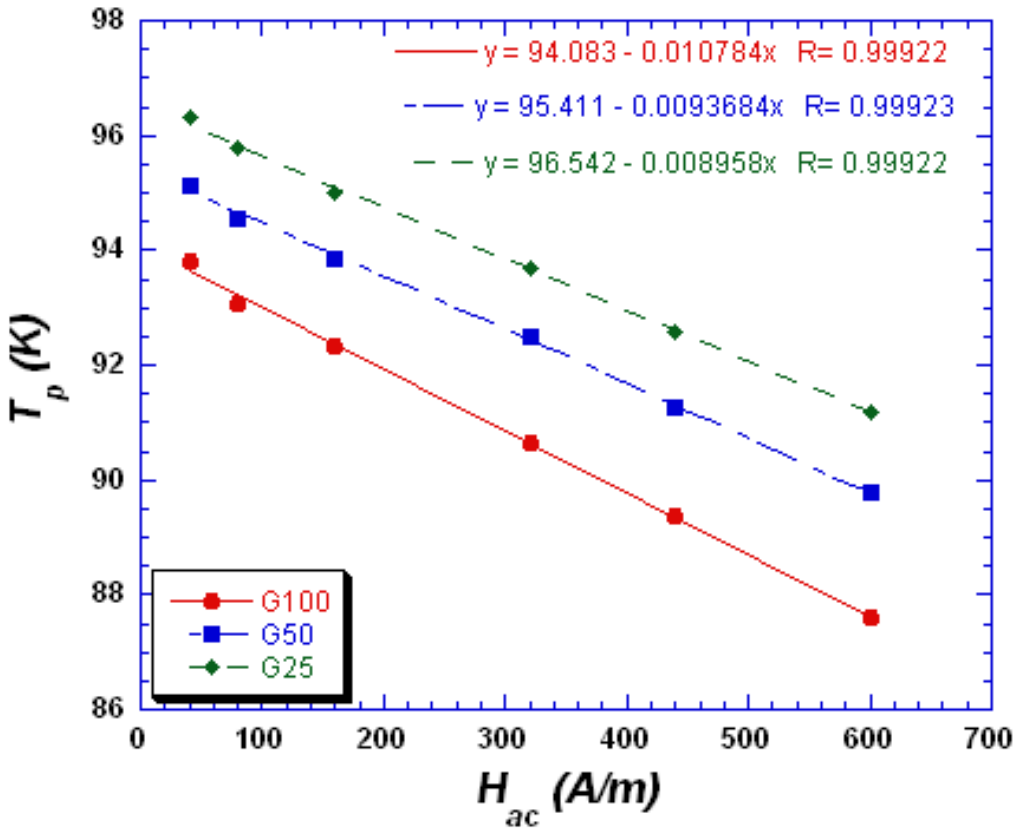

Figure 4. Intergranular peak temperature as a function of ac magnetic field amplitude for silver wrapped $Bi_{1.7}Pb_{0.35}Sr_{1.9}Ca_{2.1}Cu_3O_y$ annealed at 830 $^\circ C$ for 48 h with cooling rate of (a) 25 $^\circ C$ /h , (b) 50 $^\circ C$ /h and (c) 100 $^\circ C$ /h samples.

We have studied the peak temperature dependence as a function of ac magnetic field, H_{ac}, in order to investigate the effect of cooling rates on the inter-granular pinning force. As can be seen from Fig. 5 a linear dependence of T_p as a function of H_{ac} is observed for all the samples. Müller critical state model assumes a magnetic flux independent pinning force densities, and α_J and α_g for inter- and intra-granular vortices described by the relation [23]:

$$T_p = T_{p0} - T_{p0} U^{1/2} H_{ac} \qquad (4)$$

where U is $\left[\frac{\mu_0 \mu_{eff}(0)}{2a\alpha_J(0)}\right]$, a is the length of the samples, $\mu_{eff}(0)$ is the effective permeability of the ceramic, and $\alpha_J(0)$ is the inter-granular pinning force density. From a least squares fit of this expression (Eq.(4)) to the data T_{p0} and U were extracted for all samples. The values of T_{p0} decreased from 97 to 94 K while U increased with increasing cooling rates. This means that the values of $\alpha_J(0)$ decreases with increasing cooling rates, being consistent with our transport critical current density measurement such as Jc is decreased with increasing cooling rates. A decreasing trend in pinning force of the samples with increasing cooling rates is attributable to grater voids and defects.

The temperature dependence of inter-granular critical current density, $J_c(T_p)$, is often determined via the temperature dependence of the inter-grain maximum in the imaginary part, $\chi''(T)$ of the ac susceptibility using the Bean model [24,25]. $J_c(T_p)$ is calculated for our samples using the relation $J_c(T_p) = H_a/a$ for the sample having cross section of the rectangular bar shaped, like 2ax2b where a < b. $J_c(T_p)$ is the inter-granular current density and Ha is the amplitude of applied field at T_p. The determined $J_c(T_p)$ at 92 K for the samples is determined to be 50 A/cm^2 for G25, 35 A/cm^2 for G50 and 14 A/cm^2 for G100 sample. The value of $J_c(T_p)$ increases with decreasing cooling rate. This result is consistent with present transport critical current density measurements. Moreover, we observed the same evidence for this behavior in ρ-T transport measurements in the samples such as T_c decreases with increasing cooling rates.

4. Conclusion

Changing the cooling rate showed a remarkable effect on the transport properties, lattice parameter c and hole concentration of the silver sheathed bulk samples. The values of J_c, T_c, lattice parameter c and p of the samples were decreased with increasing cooling rate. The temperature dependence of the electrical resistivity is linear in the normal state and room temperature resistivity increased with increasing cooling rate. From ac susceptibility measurements, it is observed that T_p shifts slightly to lower temperature with increasing ac field amplitude and cooling rates. The imaginary part of susceptibility measurement is used to calculate the $J_c(T_p)$ using Bean model and the $\alpha_J(0)$ using Müller critical state model. It is observed that the both $J_c(T_p)$ and $\alpha_J(0)$ were decreased with increasing cooling rates. Thus, the inter-granular properties of the G25 sample are better than that of the G100 sample under low external ac magnetic fields.

Acknowledgements

This work is supported partly by the Scientific and Technological Council of Turkey (Project No: 104T325) and partly the Turkish State Planning Organization (DPT) (Project No: 2004K120200).

References

[1] Calzona V Cimberle M R Ferdeghini C Putti M Siri A S 1989 *Physica C* **157** 425
[2] Müller K H Macfarlane J C Driver R 1991 *Physica C* **203** 178
[3] Pop A V 1999 *Supercond. Sci. Tecnol.* **12** 672
[4] Pop A V Ilonca G Ciurchea D Ye M Geru I I Kantser V G Todic M Delteur R 1996 *J. Alloys Comp.* **116** 241.
[5] Belenli I *D. Phil. Thesis University of Oxford* 1993
[6] Parrell J A Larbalestier D C 1996 *Appl. Phys. Lett.* **69** 2915
[7] Lelovic M Deis T Eror N G Balachanran U Haldar P 1996 *Supercond. Sci. Technol.* **9** 965
[8] Terzioglu C Ozturk O Kilic A Gencer A Belenli I 2006 *Physica C* **434** 153
[9] Ozturk O Yegen D Yilmazlar M Varilci A Terzioglu C 2007 *Physica C* **451** 113
[10] Chiu C W Meng R L Gao L Huang Z J Chen F and Xue Y Y 1993 *Nature* **365** 323
[11] Halim S A Khawaldeh S A Mohammed S B Azhan H 1999 *Materials Chemistry and Physics* **61** 251
[12] Terzioglu C Yegen D Yilmazlar M Görür O Akdogan M Varilci A 2007 *J. Mater. Sci.* **42** 4636
[13] Bean C P 1964 Rev. Mod. Phys. 36 31
[14] Jean F Collin G Andrieux M Blanchard N Forget A Rousseau S and Marucco J F 2003 *Physica C* **345** 384
[15] Belenli I and Turkoglu O 2003 *Supercond. Sci. Technol.* **39** 16
[16] Tetenbaum M Maroni V A 1996 *Physica C* **260** 71
[17] Persland M R Tallon J L Buckley R G Liu R S Floer N E 1991 *Physica C* **176** 95
[18] Terzioglu C Yilmazlar M Ozturk O Yanmaz E 2005 *Physica C* **423** 119
[19] Aksan M A Yakinci M E 2004 *J. Alloys and Compounds* **385** 33

[20] Müller K H Nikolo M Savvides N Driver R Kajimura K Hayakawa H (Eds.) 1991 *Advances in Superconductivity III Springer Verlag Tokyo* p. 119.
[21] Clim J R 1991 *Physica C* **50** 153-155.
[22] Müller K H Collocott S J Driver R and Savvides N 1991 *Supercond. Sci. Technol.* **4** 325-327
[23] Müller K H Matthews D N and Driver R 1992 *Physica C* **191** 339
[24] Babic E Drobac D Horvat J Marohnic Z and Prester M 1989 *J. Less. Comm. Mat.* **151** 89
[25] Gomory F and Lobotka P 1988 *Solid State Commun.* **66** 645